RESEARCH ACTIVITIES

Theoretical and Computational Molecular Science

It is our goal to develop theoretical and computational methodologies that include quantum mechanics, statistical mechanics, and molecular simulation in order to understand correctly the structures, reactivities, and functions of molecules in gas, solution, and condensed phases as well as in nano- and bio-systems.

Theoretical Study and Design of Functional Molecules: New Bonding, Structures, and Reactions

Department of Theoretical and Computational Molecular Science
Division of Theoretical Molecular Science I

NAGASE, Shigeru	Professor
CHOI, Cheol Ho	Visiting Associate Professor*
JANG, Joonkyung	Visiting Associate Professor
OHTSUKA, Yuki	Assistant Professor
ISHIMURA, Kazuya	Technical Associate†
KATOUDA, Michio	Post-Doctoral Fellow
GAO, Xingfa	Post-Doctoral Fellow
GUO, Jing-Doing	Post-Doctoral Fellow
MIZOROGI, Naomi	Post-Doctoral Fellow‡
WANG, Lu	Post-Doctoral Fellow
SUTCLIFFE, Brian	Visiting Scientist§
KIM, Tae-Rae	Graduate Student‖
YAMADA, Mariko	Secretary
KONDOU, Naoko	Secretary

In theoretical and computational chemistry, it is an important goal to develop functional molecules prior to or in cooperation with experiment. Thus, new bonds and structures provided by heavier atoms are investigated together with the reactivities. In addition, chemical modification and properties of large molecules are investigated to develop functional nanomolecular systems. Efficient computational methods are also developed to perform reliable quantum chemistry calculations for small and large molecular systems.

1. Projector Monte Carlo Method Based on Configuration State Functions. Test Applications to the H_4 System and Dissociation of LiH[1)]

The diffusion Monte Carlo (DMC) method, also called the projector Monte Carlo (PMC) method, has attracted a lot of attention because of its high accuracy and high parallel efficiency. The parallel DMC programs have been developed and applied to various systems. However, the DMC method has an important fermion sign problem because electrons are treated as particles, and the accuracy depends strongly on the nodes of trial wave functions because the fixed-node approximation is generally used to avoid the fermion sign problem. In addition, the accuracy is not always improved systematically even if the nodes of trial functions are generated at high levels of theory. It has been shown that the trial nodes are improved using variational Monte Carlo techniques. However, it is also important to develop a quantum Monte Carlo method that does not require the nodes of trial wave functions.

Thus, we have developed a new PMC method by using configuration state functions (CSFs), spin-adapted linear combinations of Slater determinants, as walkers, to avoid the fermion sign problem (the name "PMC" is used instead of "DMC" because the diffusion equation is not used apparently in the PMC-CSF method). In the PMC-CSF method, new theory and effective calculation algorithm are developed and tested by making a simple program that can treat up to 4 electrons. The accuracy of the PMC-CSF method depends on the basis sets constructing CSFs, but is systematically improved, regardless of trial functions, by increasing the number of walkers. As verified by test applications to the H_4 and LiH systems, full-CI (configuration interaction) energies are obtainable as a limit for a given basis set (Figure 1).

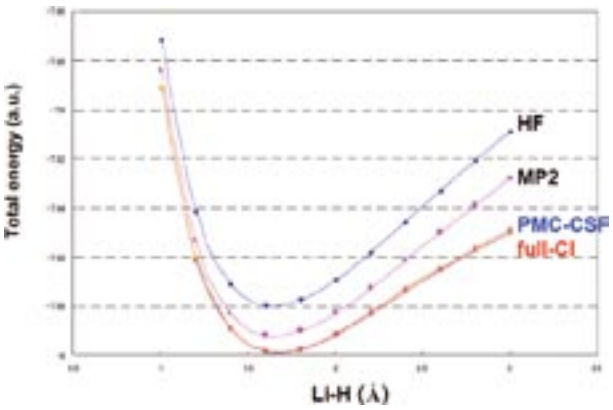

Figure 1. The dissociation of the LiH moilecule.

Obviously, the PMC-CSF method becomes highly accurate by enhancing the quality of basis sets. Unlike conventional CI calculations, no diagonalization of matrices is necessary and important CSFs are effectively selected for the PMC-CSF method. In addition, the PMC-CSF method shows good parallel efficiency, as shown in Table 1.

Table 1. Elapse time (in second) and speedup of the PMC-CSF parallel calculations of the H_4 system.

CPU	1	2	4	8
Time	3999	2010	1008	511
Speedup	1.00	1.99	3.97	7.82

We are now developing a general program suitable high parallel calculations and applicable to large molecules.

2. Chemical Modification of Endohedral Metallofullerenes[2–5)]

The reactivities and chemical modification of endohedral metallofullerenes are of considerable interest in developing functional nanomolecules. Addition of adamantylidene to $La_2@C_{78}$ takes place at the [5,6] and [6,6] positions around the pole and equator of $La_2@C_{78}$. The Addition to $M_2@C_{80}$ (M = La and Ce) makes the two metal atoms collinear with the spiro carbon of the 6,6-oen adduct. Bissilylation of $Ce_2@C_{78}$ affords regioselectively the 1,4-adduct in which the two Ce atoms stand still by facing toward the hexagonal rings at the equator. Addition of adamantylidene to $La_2@C_{72}$ (that does not satisfy the isolated pentagon rule) mainly takes place at the fused pentagons because of the high surface curvature.

3. Nanographenes and BN Analougues: Ground Electronic States and Energy Gap Engineeering[6)]

Graphene has attracted great interest as the new generation of carbon electronics. The lack of an energy gap prevents using graphene in carbon nanoelectronics. It is very important to engineer the band gap by patterning and cutting the graphene sheet into rectangular shapes. Thus, carbon nanographenes (CNGs) were theoretically investigated together with boron nitride nanographenes (BNNGs). As the size of CNGs increases, the HOMO–LUMO energy gaps decrease with a direct inverse dependence on the length of zigzag edges, CNGs with long zigzag edges having open-shell singlet ground states. In contrast, the energy gaps of BNNGs have a weak size-dependence; all BNNGs have closed-shell singlet ground states and those with long zigzag edges have slightly larger energy gaps. CNGs with long zigzag edges are less favorable energetically than their structural isomers with long armchair edges, while BNNGs have the opposite preference. Chemical modifications that change the long zigzag edge into armchair type can efficiently stabilize the kinetically unstable CNGs (with open-shell singlet ground states) and modify their energy gaps.

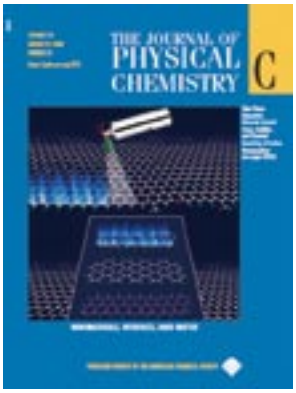

References

1) Y. Ohtsuka and S. Nagase, *Chem. Phys. Lett.* **463**, 431–434 (2008).
2) B. Gao, H. Nikawa, T. Nakahodo, T. Tsuchiya, Y. Maeda, T. Akasak, H. Sawa, Z. Slanina, N. Mizorogi and S. Nagase, *J. Am. Chem. Soc.* **130**, 983–989 (2008).
3) M. Yamada, C. Someya, T. Wakahara, T. Tsuchiya, Y. Maeda, T. Akasak, K. Yoza, E. Horn, M. T. H. Liu, N. Mizorogi and S. Nagase, *J. Am. Chem. Soc.* **130**, 1171–1176 (2008).
4) M. Yamada, T. Wakahara, T. Tsuchiya, Y. Maeda, M. Kako, T. Akasaka, K. Ypza, E. Horn. N. Mizorogi and S. Nagase, *Chem. Commun.* 558–560 (2008).
5) X. Lu, H. Nikawa, T. Nakahodo, T. Tsuchiya, M. O. Ishitsuka, Y. Maeda, T. Akasaka, M. Toki, H. Sawa, Z. Slanina, N. Mizorogi and S. Nagase, *J. Am. Chem. Soc.* **130**, 9129–9136 (2008).
6) X. Gao, Z. Zhou, Y. Zhao, S. Nagase, S. B. Zhang and Z. Chen, *J. Phys. Chem. C* **112**, 12677–12682 (2008).

* Present Address; Department of Chemistry, Kyungpook National University, Taegu 702-701, Korea
† Present Address; Toyota Central R&D Labs., Inc, Nagakute, Aichi 480-1192
‡ Present Address; Center for Tsukuba Advanced Research Alliance, University of Tsukuba, Tsukuba, Ibaraki 305-8577
§ Present Address: School of Chemistry, Seoul National University, Seoul 151-747, Korea
|| Present Address; Faculte des Sciences, Universite Libre de Bruxelles, Bruxelles 1050, Belgium

Electronic Structure and Electron-Nuclear Dynamics of Molecules in Contact with an Electron Reservoir

Department of Theoretical and Computational Molecular Science
Division of Theoretical Molecular Science I

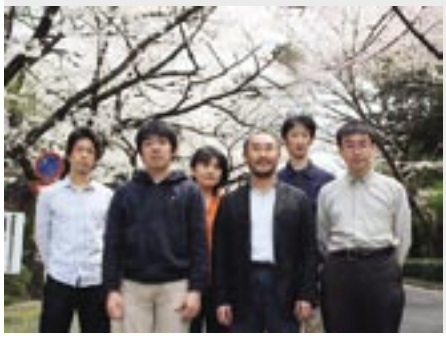

NOBUSADA, Katsuyuki	Associate Professor
YASUIKE, Tomokazu	Assistant Professor
KUBOTA, Yoji	Post-Doctoral Fellow
NODA, Masashi	Post-Doctoral Fellow
SHIRATORI, Kazuya	Graduate Student
IWASA, Takeshi	Graduate Student
YAMADA, Mariko	Secretary

Electronic structures and electron dynamics of molecules or nanostructured materials in contact with an electron reservoir play important roles in heterogeneous catalysis, surface photochemistry, and also electrochemistry. We have developed theoretical methods to calculate electronic structures of adsorbate-surface and electrochemical systems. We have also investigated exciton transfer dynamics in an array of quantum dot.

1. Open-Boundary Cluster Model for Calculation of Adsorbate-Surface Electronic States[1)]

We have developed a simple embedded-cluster model approach to investigate adsorbate-surface systems. In our approach, the physically-relevant subsystem is described as an open-quantum system by considering a model cluster subject to an outgoing-wave boundary condition at the edge. This open-boundary cluster model (OCM) is free from artificial waves reflected at the cluster edge, and thus the adsorbate properties computed with the OCM are almost independent of the model cluster size. The exact continuous density of states (DOS) of a 1D periodic potential model is shown to be precisely reproduced with the OCM. The accurate DOS leads to an appropriate description of adsorbate-surface chemical bonding. Moreover, the open-boundary treatment of the OCM allows us to evaluate the electron-transfer rate from the adsorbate to the surface, whereas the conventional cluster model does not give any information about such a dynamical process.

2. Quasi-Diabatic Decoupling of Born-Oppenheimer Potential Energy Curves for Adsorbate-Metal Surface Systems[2)]

We have applied the open-system treatment, recently developed by the authors, to a simple adsorbate-metal surface model potential. The open-system treatment is found to give a quasi-diabatic representation where the adsorbate electronic states cross the metal ones in the manifold consisting of the Born-Oppenheimer potential energy curves of the whole system. On the obtained quasi-diabatic curves, one can effectively follow time propagation of a nuclear wave packet. The computed propagation has revealed that the formation of a metastable adsorbate leads to the coherent vibrational motion of the neutral adsorbate as well as the desorption induced by electronic transitions.

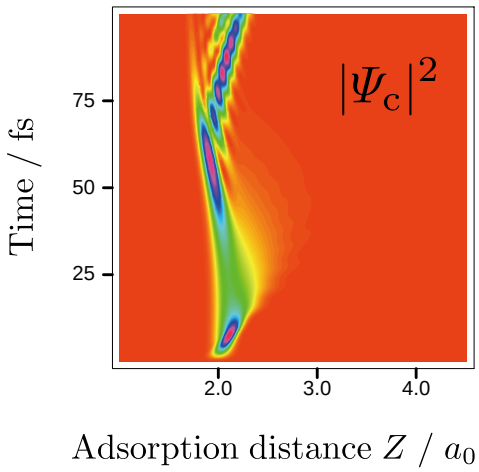

Figure 1. Nuclear wave-packet motion of the neutral adsorbate.

3. Exciton Transfer in Quantum Dot Arrays: Comparison of Eigenbasis and Site Basis Representations[3)]

We discuss differences between eigenbasis and site basis representations for models of exciton transfers in an array of quantum dots. The exciton relaxation processes are well described by the master equation in the eigenbasis representation. The site-basis evolution equation up to the second order of the interdot interaction is straightforwardly derived from the eigenbasis equation by using perturbation theory when the interaction is sufficiently small compared with the energy difference between the exciton states in each quantum dot. Although the higher order site basis equations can be derived similarly, the resultant equations are too complicated to use in the actual calculations. The master equation in the eigenbasis representation has several advantages over the site basis one: (i) the system described in terms of the eigenbasis representation can evolve into thermal equilibrium because the equation satisfies the detailed balance, (ii) the site basis equation does not reasonably describe the exciton state trapped in a local energy minimum at very low temperature, and (iii) it is computationally less demanding to carry out the eigenbasis evolution equation.

4. Development of Finite-Temperature Density Functional Approach to Electrochemical Reactions[4)]

We present a computational method to calculate the electronic states of a molecule in an electrochemical environment. The method is based on our recently developed finite-temperature density functional theory approach to calculate the electronic structures at a constant chemical potential. A solvent effect is treated at the level of the extended self-consistent reaction field model, which allows considering a nonequilibrium solvation effect. An exchange-correlation functional with a long-range correction is employed in this calculation, because the functional is adjusted so that the derivative discontinuity of energy with respect to a number of electrons could be satisfied. It has been found that the derivative discontinuity condition plays a crucial role in an electrochemical system. The computational results are presented for a reaction of $NO^+ + e^- \rightleftarrows NO$ in chemical equilibrium. Owing to the improvement in the solvation effect and the exchange-correlation functional, the calculated activation free energy is in good agreement with experimental results.

5. Oligomeric Gold Clusters with Vertex-Sharing Bi- and Triicosahedral Structures[5)]

We present density functional studies of geometric and electronic structures of a gold cluster compound $[Au_{25}(PH_3)_{10}(SCH_3)_5Cl_2]^{2+}$ (**1**). The cluster has a unique geometric structure consisting of two icosahedral Au_{13} clusters bridged by methanethiolates sharing a vertex gold atom and terminated by chlorine atoms. This structure is very close to the biicosahedral gold cluster $[Au_{25}(PPh_3)_{10}(SC_2H_5)_5Cl_2]^{2+}$ reported in the recent experiment. We further demonstrate that a vertex-sharing triicosahedral gold cluster $[Au_{37}(PH_3)_{10}(SCH_3)_{10}Cl_2]^+$ is also achieved through bridging with the methanethiolates. A comparison between the absorption spectra of the bi- and triicosahedral clusters shows that the new electronic levels due to each oligomeric structure appear sequentially, whereas other electronic properties remain almost unchanged compared to the individual icosahedral Au_{13} cluster

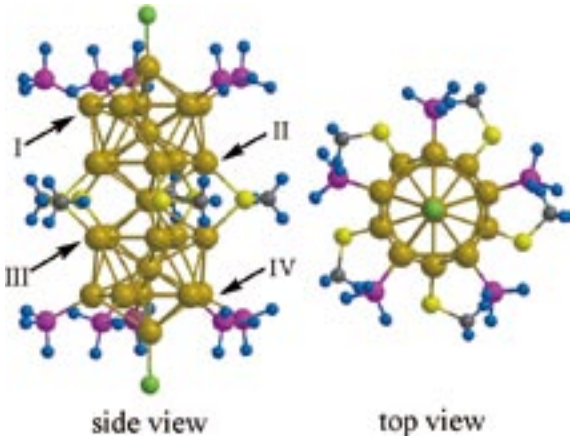

Figure 2. Side and top views of the optimized structure of **1**. The colored balls represent constituent atoms: Au (gold), S (yellow), C (gray), H (blue), P (magenta), Cl (green).

References

1) T. Yasuike and K. Nobusada, *Phys. Rev. B* **76**, 235401 (12 pages) (2007).
2) T. Yasuike and K. Nobusada, *Chem. Phys. Lett.* **457**, 241–245 (2008).
3) Y. Kubota and K. Nobusada, *J. Chem. Phys.* **129**, 094704 (7 pages) (2008).
4) K. Shiratori and K. Nobusada, *J. Phys. Chem. A* **112**, 10681–10688 (2008).
5) K. Nobusada and T. Iwasa, *J. Phys. Chem. C* **111**, 14279–14282 (2007).

Advanced Electronic Structure Theory in Quantum Chemistry

Department of Theoretical and Computational Molecular Science
Division of Theoretical Molecular Science I

YANAI, Takeshi	Associate Professor
KURASHIGE, Yuki	Assistant Professor
MIZUKAMI, Wataru	Graduate Student
YAMADA, Mariko	Secretary

Aiming at predictive computational modelings of molecular electronic structures with *ab initio* quantum chemistry calculations, our scientific exploration is to establish a cutting-edge theoretical methodology that allows one to compute accurately and efficiently the complex electronic structures where the substantial multireference character in the wave functions has to be handled for the qualitative and quantitative descriptions. Our resultant works to be reported here are (1) to develop a new type of the multireference correlation model named Canonical Transformation (CT) theory, which can efficiently describe short-range dynamic correlation on top of the multi-configurational staring wave function, and (2) to construct the extensive complete active space self-consistent field (CASSCF) method combined with *ab initio* density matrix renormalization group (DMRG) method for making unprecedentedly larger active spaces available for the CASSCF calculations. These two pivotal developments are tailored to eventually be incorporated for solving large-scale multi-reference electronic structure problems.

1. Large-Scale Complete Active Space Self-Consistent Field (CASSCF) with *ab initio* Density Matrix Renormalization Group (DMRG): "DMRG-CASSCF"[1)]

To perform the large-scale multireference calculations with CT or other multireference methods, the extensively active-spaced reference wave functions where a large number of active electrons are highly (or fully) correlated within the selected active orbitals must be found. The CASSCF method provides the most desirable, optimal reference wave functions, in which the static correlations are effectively captured with the relaxed active orbitals that are optimized self-consistently by energy minimization at a high computational cost. We have developed the large-scale CASSCF method by implementing orbital optimization in the extant DMRG implementation to further allow the self-consistent improvement of the active orbitals, as is done in the standard CASSCF calculations. By virtue of the compact nature of the DMRG wavefunction, this now enables us to handle unprecedentedly larger active space than are possible with the traditional CASSCF. The further feasibility comes concomitantly with a new development of the parallelized orbital optimization allowing for high-quality basis representations of the orbitals. We have named the resulting method DMRG-CASSCF (Figure 1).

Figure 1. Schematic sketch of DMRG-CASSCF implementation. CI and MO coefficients are determined with the alternating two-step algorithm. The new development has realized the efficient computation of 1-, 2-RDMs of DMRG wavefunction, taking advantage of the compact structure of DMRG ansatz.

As applications, we have used our DMRG-CASSCF method to study the low-lying excitations of polyenes from C_8H_{10} to $C_{24}H_{26}$ (11 conjugated bonds) as well as light-harvesting pigment, β-carotene (10 conjugated bonds) with up to a CAS (24e,24o) of full π valences (Figure 2–3). The

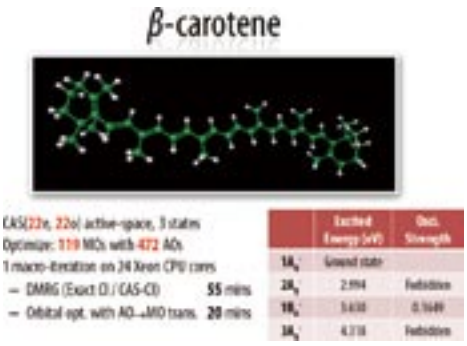

Figure 2. Details of the DMRG-CASSCF calculation for β-carotene along with excitation energies of its three dark states.

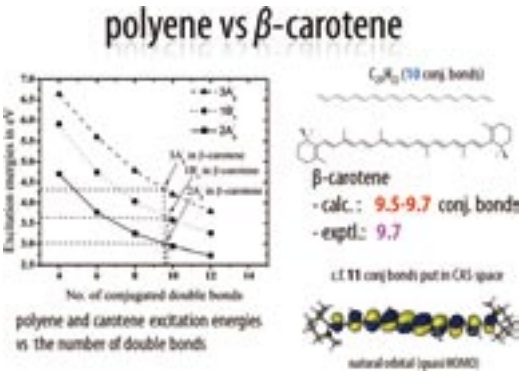

Figure 3. Carotene excitation energies of three states are fitted to polyene excitation energies. We estimated an effective conjugation length of beta-carotene to be 9.5–9.7. These numbers are in good agreement with the experimental estimation 9.7.

conjugated π-system in polyenes and substituted species such as β-carotene give rise to an unusual excitation spectrum, with "dark" electronic states lying beneath the optically allowed HOMO-LUMO transition. The electronic structure of these low-lying states lies at the heart of energy transport in system ranging from the conjugated organic semiconductors to the biological centers of light-harvesting and vision. While the relevant active space on these systems clearly consists of the conjugated π-valence orbitals, to the best of our knowledge, previous calculations have used "incomplete" π-valence space which is limited up to CAS (10e,10o) (*i.e.* 5 nominal conjugated bonds).

2. Robust Implementation of *ab initio* DMRG for Transition Metal Molecular Complexes

Our group has started an alternative implementation of *ab initio* DMRG with algorithmic improvements in which we have some new tricks in constructing operators in renormalization and subspacing Hamiltonian. The development is ongoing with a new scheme of computer parallelism for flop- and memory-distributions of DMRG operators. The development is tailored to computationally affordable applications to accurate, robust electronic structure calculations of complex transition-metal complexes, for which the conventional theoretical treatments get in trouble with entangled electronic states inherent to *d* electrons/orbitals. Figure 4 shows the recent achievement in the performances of our DMRG implementation for calculating isomerization energies of $Cu_2O_2^{2+}$ core. Our method recovers a substantial portion of the full correlation energies efficiently from correlating valence *d* electrons of two Cu atoms with other valences of Cu and O atoms on equal footing

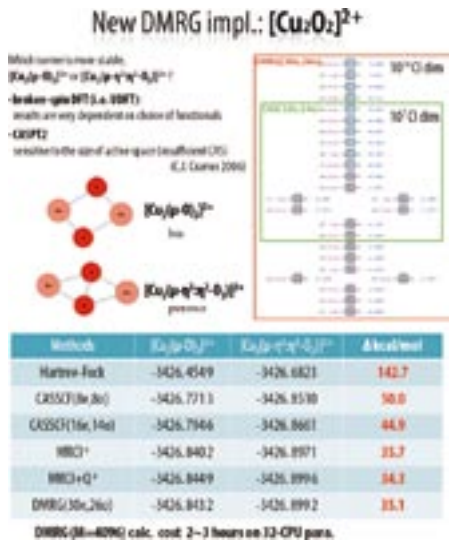

Figure 4. Isomerization energies of $Cu_2O_2^{2+}$ core between bis and peroxo structures by various methods including our new implementation of DMRG. The new, efficient implementation carried out the fully correlated electronic structure calculations.

3. Canonical Transformation (CT) Theory for Efficient Multireference Method[2)]

We have been developing a many-body technique based on canonical transformation (CT) for realizing large-scale multireference calculations for the purpose of attaining the chemical accuracy, for which dynamical correlations are described by using cluster expansion on top of muticonfigurational setting (*e.g.* DMRG-CASSCF). We are working on extending the implementation to the wider applications in terms of tractable size of molecules of target. The ongoing reimplementation fixes some of problems in the extant implementation that relies on infinite computer memory. Figure 5 presents the recent application of CT to the description of an energy curve along the isomerization coordinate between bis and peroxo cores of $Cu_2O_2^{2+}$.

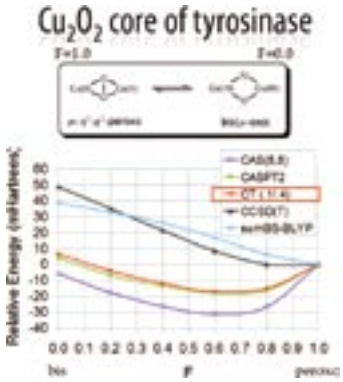

Figure 5. Relative energy curves along the isomerization coordinate between bis and peroxo cores. The difficulty in describing electronic structure of this isomerization arises in maintaining the balanced description of rapidly changing dynamic and static correlation effects and a varying degree of biradical character along the coordinate.

References

1) D. Ghosh, J. Hachmann, T. Yanai and G. K-L. Chan, *J. Chem. Phys.* **128**, 144117 (2008).
2) T. Yanai and G. K-L. Chan, *J. Chem. Phys.* **127**, 104107 (2007).
3) H. Sekino, Y. Maeda, T. Yanai and R. J. Harrison, *J. Chem. Phys.* **129**, 034111 (6 pages) (2008).

Developing the Statistical Mechanics Theory of Liquids in Chemistry and Biophysics

Department of Theoretical and Computational Molecular Science
Division of Theoretical Molecular Science II

HIRATA, Fumio	Professor
CHONG, Song-ho	Assistant Professor
YOSHIDA, Norio	Assistant Professor
MARUYAMA, Yutaka	Post-Doctoral Fellow
MIYATA, Tatsuhiko	Post-Doctoral Fellow
ISHIZUKA, Ryosuke	Post-Doctoral Fellow
PHONGPHANPHANEE, Saree	Graduate Student
KIYOTA, Yasuomi	Graduate Student
YAMAZAKI, Yumi	Secretary
KATAYAMA, Naoko	Secretary
KONDO, Naoko	Secretary
YAMADA, Mariko	Secretary

We have been exploring the chemical and biological processes in solutions, based on the statistical mechanics of liquids, especially, on the integral equation theory of molecular liquids or the "RISM" and "3D-RISM" theories.[1–3] Such exploration can be realized by combining the statistical mechanics theories with the other theoretical methods in the molecular science, which describes the different aspects of the physics such as the quantum processes and the liquid dynamics.

Our recent attention is focused on the "molecular recognition" and "fluctuation" of bio-molecules, which are the two key-processes in the living system. For examples, for an enzymatic reaction to take place, substrate molecules should be accommodated by the enzyme. The process is nothing but the molecular recognition which is regulated by the solvation free energy of the enzyme-substrate (ES) complex, and by the structural fluctuation of the protein.

1. A Water Molecules Identified as a Substrate of Enzymatic Hydrolysis of Cellulose: A Statistical-Mechanics Study[4]

Among the technologies to utilize the solar energy, the cellulose decomposition due to the enzymatic hydrolysis is getting the highest expectation, because the available resource on the earth is essentially inexhaustible, and the reaction proceeds in natural conditions without using precious metals as a catalyst. However, there is a high barrier to be cleared for the technology to be established as the ultimate substitute for the fossil fuel, that is, how to improve the efficiency of the enzyme. In order to improve the efficiency, one has to clarify the mechanism of the enzymatic hydrolysis reaction. We have started to investigate the problem last year based on the 3D-RISM theory, taking a cellulase-cellohexaose complex as an example.

There are two models proposed by experimentalists for the mechanism of the enzymatic hydrolysis reaction of cellulose, the inverting and retention processes, which can be distinguished by the distance between the two catalytic residues, and by the position of a water molecule as the substrate of the reaction. In our particular example of the Cel44A-cellohexaose complex, the distance is ~5.5 Å for the retention process, whereas that for the inverting process is ~10.0 Å. The water molecule in the inverting process can make hydrogen bonds only with one of the catalytic residues due to the large separation between the residues, while the molecule can make hydrogen-bonds with the both catalytic residues in the retention process (Figure 1).

Shown in Figure 2 is our result for the distribution of water molecules (yellow and green spots) around the active site of the ES-complex. We have identified the water molecule (colored green) as the substrate of the reaction, since the peak of which is distinctly high among other spots. The water molecule is apparently making hydrogen-bonds with the two catalytic residues, Glu186 and Glu359. This is a clear support to the retention mechanism explained above.

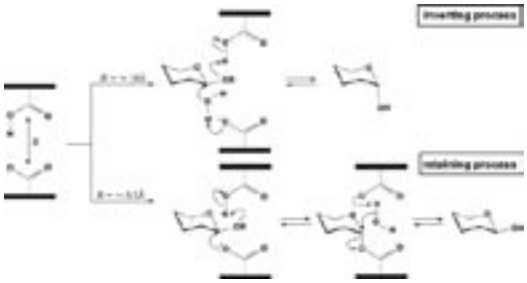

Figure 1. Schematic description of enzymatic hydrolysis of cellulose.

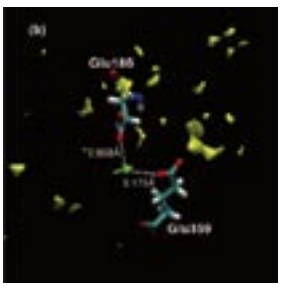

Figure 2. Distribution of water around the active site of the ES-complex.

2. RISM-SCF Study of Temperature and Solvent Dependence of the Free-Energy Surface of the Intramolecular Electron-Transfer[5)]

The free energy surfaces along the intramolecular electron transfer reaction of 1,3-dinitrobenzene radical anion in acetonitrile and methanol are investigated with the reference interaction site model self-consistent field theory. The scheme of the intramolecular electron transfer reaction of 1,3-dinitrobenzene radical anion is shown in figure 3. Although acetonitrile and methanol have similar values of the dielectric constant, the free energy profiles are quite different. In the methanol solution, the charge is strongly localized on one of the nitrile substituents due to a strong hydrogen bond between 1,3-dinitrobenzene and the solvent, while the polarization is not so large in the case of acetonitrile. The temperature dependence of the reorganization energy, the coupling strength and the activation barrier are evaluated in both acetonitrile and methanol. The reorganization energy and the activation barrier decrease with increasing temperature for both cases. The electronic coupling strength also shows similar tendency in the temperature dependence: it increases with increasing temperature in the both solvents, but with different rates. The behavior is explained in terms of the strong polarization induced by the hydrogen bond between solute and solvent in the methanol solution.

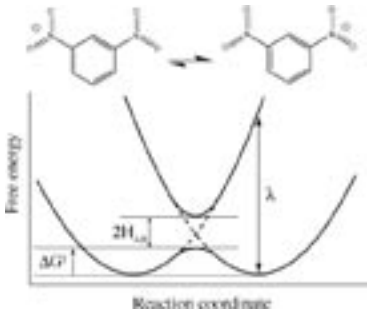

Figure 3. The scheme of the intramolecular electron transfer reaction of 1,3-dinitrobenzene radical anion.

3. On the Proton Exclusion of Aquaporins: A Statistical Mechanics Study[6,7)]

The proton exclusion from aquaporins (AQPs) is one of the most important questions to be solved in the fields of biochemistry, medicine and pharmacology. Although the channels are extremely permeable for water, approximately a billion molecules per second pass through the channel, protons are strictly excluded from the permeation. The mechanism should be readily examined if one can calculate the distribution of the hydronium ion in the channel. The information of the hydronium-ion distribution in the channel may also be useful for examining the possibility of the proton-jump mechanism, because a proton should be existing most likely in the form of the hydronium ion except for the moment of barrier crossing. In this study, we apply the 3D-RISM theory to AQP1 and GlpF for elucidating the proton exclusion from those channels.

In Figure 4, the contour map of the electrostatic potential due to the channel atoms, the 3D-distribution of the water and of hydronium ions, and the one-dimensional profile of the distribution of the solution components are depicted along the channel axis. In both channels, water distributes continuously throughout the channel, while the distribution of hydronium ions is intermitted by gaps due to the electrostatic repulsion originated from the positive charges in the channels. The gap is very large in the case of AQP1, extending from R197 to the NPA region. From the results, we can readily conclude in the case of AQP1 that protons are excluded from permeation primarily due to the electrostatic repulsion inside channel. On the other hand, in the case of GlpF, the results leave slight possibility for proton to permeate through the gap around R206 by the proton jump mechanism. However, the mechanism does not work entirely through out the channel due to the formation of the bipolar orientation at the NPA region. So, a proton has small but discernable conductivity in GlpF through the combined mechanism of the proton jump and the diffusion of hydronium ions in accord with the experiment.

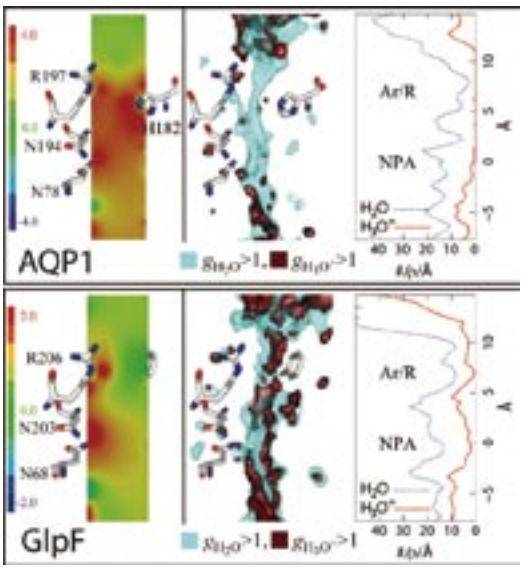

Figure 4. The distribution functions of water and hydronium ion in aquaporin channels. The contour colors show the electrostatic potential of protein in esu unit.

References

1) F. Hirata, *Molecular Theory of Solvation*, Kluwer; Dordrecht, Netherlands (2003).
2) A. Kovalenko and F. Hirata, *J. Chem. Phys.* **110**, 10095–10112 (1999).
3) T. Imai, R. Hiraoka, A. Kovalenko and F. Hirata, *J. Am. Chem. Soc. (Communication)* **127**, 15334–15335 (2005).
4) Y. Ikuta, S. Karita, Y. Kitago, N. Watanabe and F. Hirata, *Chem. Phys. Lett.* **465**, 279–284 (2008).
5) N. Yoshida, T. Ishida and F. Hirata, *J. Phys. Chem. B* **112**, 433–440 (2008).
6) S. Phongphanphanee, N. Yoshida and F. Hirata, *J. Am. Chem. Soc. (Communication)* **130**, 1540–1541 (2008).
7) S. Phongphanphanee, N. Yoshida and F. Hirata, *J.Mol. Liq.* in press.

Nonequilibrium Theory of Conductors

Department of Theoretical and Computational Molecular Science
Division of Theoretical Molecular Science II

YONEMITSU, Kenji	Associate Professor
YAMASHITA, Yasufumi	Assistant Professor
MAESHIMA, Nobuya	Post-Doctoral Fellow*
MIYASHITA, Satoshi	Post-Doctoral Fellow
TANAKA, Yasuhiro	Post-Doctoral Fellow
KATAYAMA, Naoko	Secretary

When low-dimensional correlated electron systems such as organic conductors are placed in nonequilibrium environments, they sometimes show novel phenomena that never appeared in conventional conductors based on rigid bands. One example is found in the current-voltage characteristics and the field-effect characteristics caused by metal-Mott-insulator interfaces. Another example is found in photoinduced phase-transition dynamics, where the induced transient state is not reached by simply changing temperature or pressure. It is possible because the energy of a photon is much higher than thermal energies. Our theoretical researches are focused on the mechanisms of such nonlinear phenomena.

1. Suppression of Rectification at Metal–Mott-Insulator Interfaces[1)]

Charge transport through metal–Mott-insulator interfaces is studied and compared with that through metal-band-insulator interfaces. For band insulators, rectification has been known to occur owing to a Schottky barrier, which is produced by the work-function difference.

For Mott insulators, however, qualitative different current-voltage characteristics are obtained. Theoretically, we use the one-dimensional Hubbard model for a Mott insulator and attach to it the tight-binding model for metallic electrodes. A Schottky barrier is introduced by a solution to the Poisson equation. The current density is calculated by solving the time-dependent Schrödinger equation. We mainly use the time-dependent Hartree-Fock approximation and also use exact many-electron wave functions on small systems for comparison. Rectification is found to be strongly suppressed even for large work-function differences.

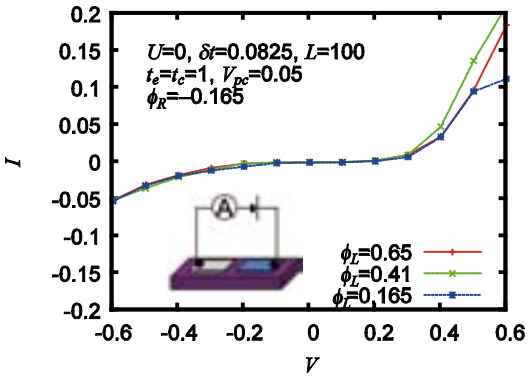

Figure 1. Current-voltage characteristics for a band insulator. Rectification is clearly seen.

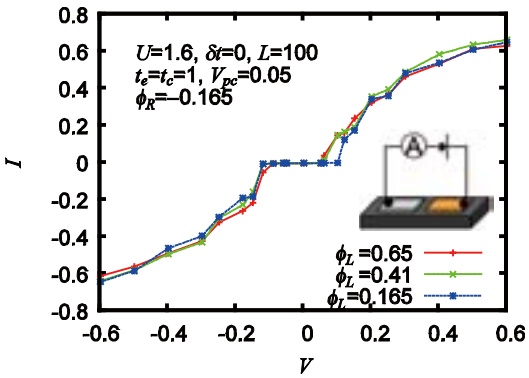

Figure 2. Current-voltage characteristics for a Mott insulator. Rectification is suppressed.

Its close relationship is shown with the fact that field-effect injections into one-dimensional Mott insulators are ambipolar. Experimentally, we fabricated asymmetric contacts on top of single crystals of quasi-one-dimensional organic Mott and band insulators. Rectification is strongly suppressed at an interface between metallic magnesium and Mott-insulating (BEDT-TTF)(F_2TCNQ).

2. Charge Order with Structural Distortion in Organic Conductors: Comparison between θ-(ET)$_2$X and α-(ET)$_2$X Salts[2)]

Charge ordering with structural distortion in quasi-two-

dimensional organic conductors θ-(BEDT-TTF)$_2$RbZn(SCN)$_4$ and α-(BEDT-TTF)$_2$I$_3$ is investigated theoretically. We use the Hartree-Fock approximation, strong-coupling perturbation theory, and exact diagonalization of a 3/4-flled extended Hubbard model for an anisotropic triangular lattice. The model includes on-site and inter-site Coulomb interactions together with Peierls-type electron-lattice couplings. We examine the effect of lattice degrees of freedom on charge order. It is found that the experimentally observed, horizontal charge order is stabilized by lattice distortion in both compounds. In particular, the lattice effect is crucial to the realization of the charge order in θ-(BEDT-TTF)$_2$RbZn(SCN)$_4$, while the peculiar band structure of α-(BEDT-TTF)$_2$I$_3$ whose symmetry is lower than that of θ-(BEDT-TTF)$_2$RbZn(SCN)$_4$ is also an important factor in α-(BEDT-TTF)$_2$I$_3$ together with the lattice distortion. For α-(BEDT-TTF)$_2$I$_3$, we obtain a transition from the metallic phase with charge disproportion to the horizontal charge order with lattice modulations, which is consistent with the latest X-ray experimental result.

3. Photoinduced Change in the Charge Ordering Pattern in (EDO-TTF)$_2$PF$_6$ with Strong Electron-Phonon Interaction[3)]

The quasi-stable state in the photoinduced phase transition for the quasi-one-dimensional quarter-filled organic conductor (EDO-TTF)$_2$PF$_6$ has been examined by ultrafast reflective measurements and time-dependent model calculations incorporating both electron-electron and electron-phonon interactions. The transient optical conductivity spectrum over a wide probe photon energy range revealed that photo- excitation induced a new type of charge-disproportionate state. Additionally, coherent and incoherent oscillations dependent on probe photon energies were found, as predicted by the calculation.

The photoinduced state has a (1010) charge separation owing to competing long-range e–e and e–anion interactions.

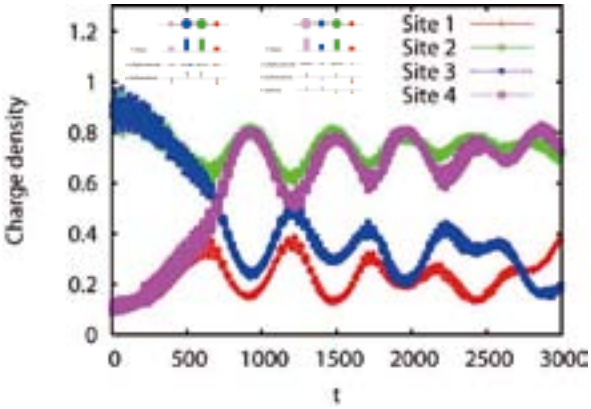

Figure 3. Time dependence of charge densities after the (0110)-charge-order ground state is photoexcited to a {0200} state.

On the low-energy side of the photoinduced peak, the transient spectrum shows irregular time dependences. It is because delocalized electrons are observed there, which are scattered by phonons on different molecules and times. Thus, the coherence is easily lost.

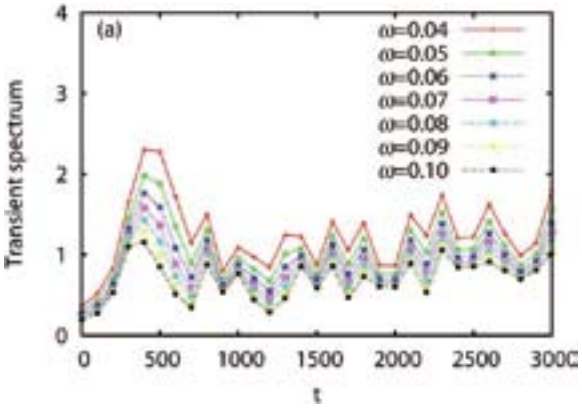

Figure 4. Time dependence of transient spectra on the low-energy side of a main peak, after photoexcitation from (0110) to {0200}.

On the high-energy side of the photoinduced peak, the transient spectrum shows coherent oscillations. It is because localized charge-transfer processes are observed there, which are governed by the instantaneous distribution of charge and displacements. The coherence is rather robust.

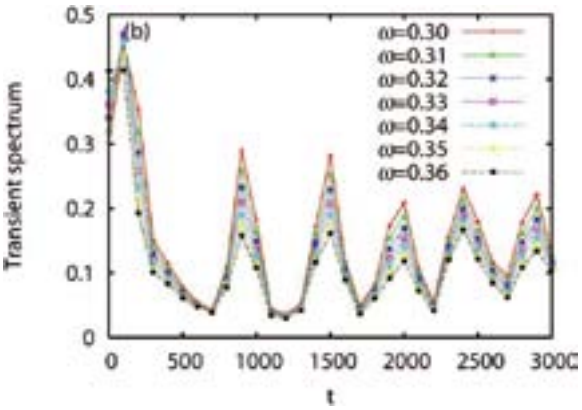

Figure 5. Time dependence of transient spectra on the high-energy side of a main peak, after photoexcitation from (0110) to {0200}.

References

1) K. Yonemitsu, N. Maeshima and T. Hasegawa, *Phys. Rev. B* **76**, 235118 (6 pages) (2007).
2) Y. Tanaka and K. Yonemitsu, *J. Phys. Soc. Jpn.* **77**, 034708 (9 pages) (2008).
3) K. Onda, S. Ogihara, K. Yonemitsu, N. Maeshima, T. Ishikawa, Y. Okimoto, X. -F. Shao, Y. Nakano, H. Yamochi, G. Saito and S. Koshihara, *Phys. Rev. Lett.* **101**, 067403 (4 pages) (2008).

* Present Address: Institute of Materials Science, University of Tsukuba, Tsukuba, Ibaraki 305-8573

Molecular Dynamics Study of Classical Complex Systems and Quantum Systems in Condensed Phase

Department of Theoretical and Computational Molecular Science
Division of Computational Molecular Science

OKAZAKI, Susumu	Professor*
YAMADA, Atsushi	Assistant Professor
MIKAMI, Taiji	Post-Doctoral Fellow
ANDOH, Yoshimichi	Post-Doctoral Fellow
FUJIMOTO, Kazushi	Graduate Student

1. Electrostatic Potential Gap at the Interface between Triethylamine and Water Phases Studied by Molecular Dynamics Simulation[1)]

Molecular dynamics calculations were carried out in order to investigate the interfacial properties of the two-phase coexistence state of the triethylamine (TEA) and water mixture, which is known to have a lower critical soluble temperature. Two kinds of initial configuration were adopted. One was a two-phase coexistence state and the other was a random mixed state of TEA and water molecules. After an equilibration calculation of several nanoseconds, the density profiles converged to the same equilibrated two-phase coexistenc state. In the equilibrated state, anisotropic orientations were observed for both molecules, which makes an electrostatic potential gap between these phases.

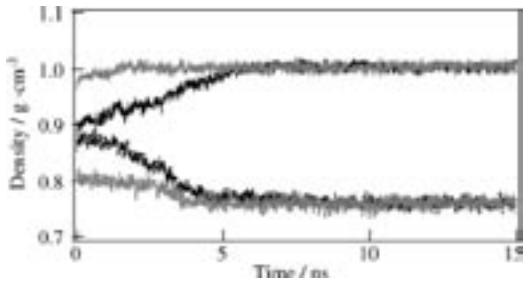

Figure 1. Time evolution of the density of the water phase (solid line) and TEA phase (dotted line) obtained from the MD calculation started from the two-phase state (gray) and from the mixed state (black).

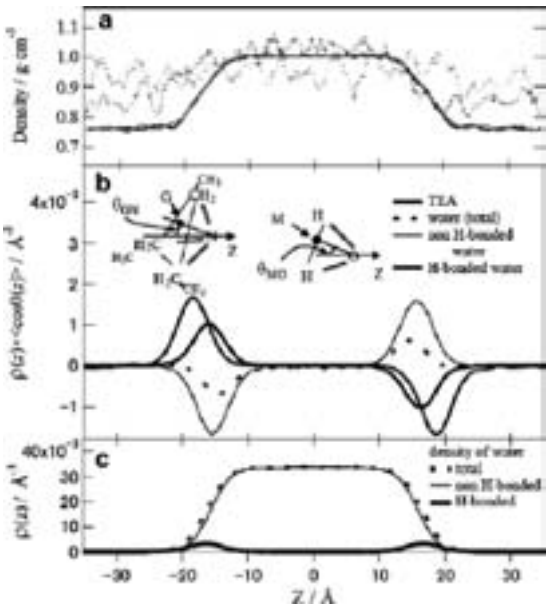

Figure 2. (a) Equilibrated density (solid line) profile calculated from the twophase state (black) and from the mixed state (gray). The corresponding density profile of the initial states is also shown with dotted lines. (b) q(*z*) A Acosha for TEA molecule (gray) and for water (black) as a function of the *z*-coordinate. Those with respect to the water molecule, hydrogen bonded (dotted) and non-hydrogen bonded molecules (thin line) to the nitrogen atom of TEA molecule are shown. Definition of hGN and hMO are also shown schematically (see text). (c) Density profile for water molecules.

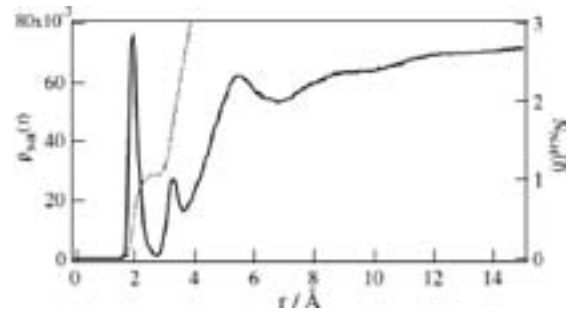

Figure 3. Pair distribution function $\rho_{N-H}(r)$ (solid line) and its running coordination number, $N_{N-H}(r)$ (dotted line), at the vicinity of the interface with a width of 10 Å.

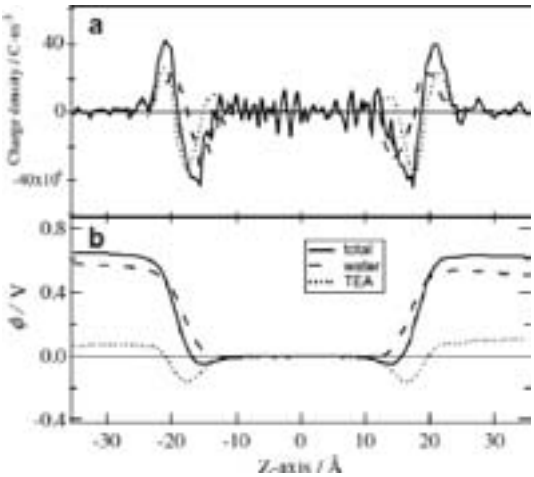

Figure 4. Charge density (a) and electrostatic potential profile (b) as a function of the *z*-coordinate. Solid line; the total system, dotted line; TEA molecule contribution and broken line: Water molecule contribution.

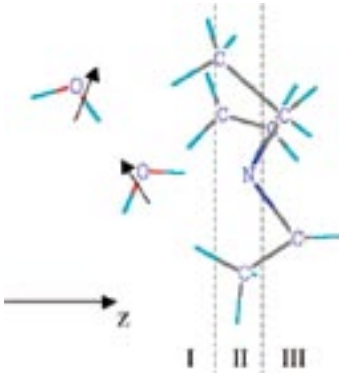

Figure 5. Schematic image of water and TEA molecules at the interface.

We have performed molecular dynamics calculations for the two-phase coexistence state of the TEA and water mixture. At the interface between the two phases, both molecules have unique orientations, which results from hydrogen bonding between TEA and water molecules. These anisotropic orientations lead to a large potential gap of 0.65 V between two phases. Additionally, resulting from the orientation of the TEA molecules, the electric potential has the minimum value in the vicinity of the interface

2. A molecular Dynamics Study of Structure and Dynamics of Surfactant Molecules in SDS Spherical Micelle[2)]

An analysis of structure and dynamics of surfactant molecules in SDS micelle is presented based on molecular dynamics calculations. Two-dimensional surface correlation function for the hydrophilic sulfur atoms as well as the bond analysis between the hydrophobic alkyl chains shows that the surfactant molecules are packed sparsely in the micelle such that they form a soccer ball-like structure characterized by the coordination number of three. The hydrophobic bond between the surfactant molecules is produced and annihilated repeatedly in a time scale of about 100 ps but disappears by their diffusion in a time scale of about 1 ns.

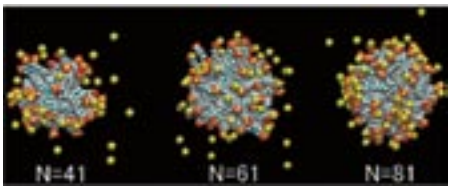

Figure 6. Snapshots of the simulated SDS spherical micelles formed in water. In the figure, water molecules are not drawn just for clarification.

References

1) S. Kajimoto, N. Yoshii, J. Hobley, H. Fukumura and S. Okazaki, *Chem. Phys. Lett.* **448**, 70–74 (2007).
2) N. Yoshii and S. Okazaki, *Cond. Matt. Phys.* **10**, 573–578 (2007).

* Present Address; Nagoya University

Theoretical Studies on Condensed Phase Dynamics

Department of Theoretical and Computational Molecular Science
Division of Computational Molecular Science

SAITO, Shinji	Professor
KIM, Kang	Assistant Professor
KOBAYASHI, Chigusa	Post-Doctoral Fellow
YAGASAKI, Takuma	Post-Doctoral Fellow
UENO, Harumi	Secretary

Liquids and biological systems show complicated dynamics because of their structural flexibility and dynamical hierarchy. Understanding these complicated dynamics is indispensable to elucidate chemical reactions and relaxation in solutions and functions of proteins. We have been investigating liquid dynamics and chemical reactions in biological systems using molecular dynamics simulation and electronic structure calculation. In addition, we have been analyzing complicated liquid dynamics using multi-dimensional spectroscopy.

1. Slow Dynamics in Random Media: Crossover from Glass to Localization Transition

The transport phenomena of fluids confined in random media is of great important in physics, chemistry, biology, and engineering, *e.g.* water in micelles or living cells. Spatial restrictions in random media can cause unusual slow dynamical properties. Recent experiments suggest that the glass transition temperature in spatially confined systems, *e.g.* a thin film or a porous media, is largely different from that in bulk, though little is understood about these phenomena.

Recently, the glass transition of hard-spheres confined in random media has intensively investigated based on the mode-coupling theory (MCT) and two notable results were predicted. First, the memory kernel in the MCT equation consists of the linear and nonlinear terms. Coupling coefficients in the memory kernel representing fluid-fluid and fluid-matrix interactions are controlled by varying fluid and matrix densities. Thus, the glass transition dynamics is characterized by two kinds of dynamics which are called the two-step type B dynamics at high fluid densities and the single-step type A dynamics at small fluid densities, respectively. Second prediction is the existence of the reentrant transition in low fluid density regime at a certain high matrix density, where delocalization of fluid particles occurs and the dynamics become faster in spite of the increase in the fluid density with a fixed matrix density.

In the present study, we carry out molecular dynamics simulations of soft sphere supercooled liquids and hard sphere liquids in random media to obtain quantitative information about dynamics over a broad range of fluid and matrix densities and the physical interpretation of the above theoretical predictions. Dynamical phase diagram of the liquid-glass transition at various fluid and matrix densities has been determined from simulations, which is well correlated with MCT's predictions. Two types of dynamics, type A and B, have been found in density correlation function, mean square displacement, non-ergodic parameter, and four-point correlation function. Furthermore, it is found that in the low fluid density at a certain high matrix density the reentrant transition exists as MCT predicts, where the delocalization of particles occur due to kick-out mechanics resulting from hopping motions of fluid particles surrounded by the random media.

2. Conformational Changes and Fluctuations of Ras

Ras superfamily is a signal transduction protein. Ras is cycled between two states of bound guanine nucleotide, the GTP- and GDP-bound states, by hydrolysis. Ras binds to effectors for regulation of cell proliferation in the GTP-bound state, whereas it is inactivated in the GDP-bound state. X-ray crystallography studies revealed conformational changes of two regions around a nucleotide binding site, switch I and switch II, in the two states. The conformational changes result from the difference of the coordinations of γ-phosphate, Gly60 and Thr35 in the two states. In addition to the conformational change between the GTP- and GDP-bound states, two states with different conformations are experimentally found in the GTP-bound state. The two states are called state 1 and state 2. The results of ^{31}P NMR show that the interconversion between states 1 and 2 is governed by the coordination between Thr35 and Mg^{2+} and that state 2 is a predominant form of H-Ras and

interacts with effectors. We investigated the conformational changes and fluctuations in the two states, states 1 and 2, in the GTP-bound state and the GDP-bound state by using molecular dynamics calculations.

We found the large difference of the secondary structure of switch I in states 1 and 2 and the GDP-bound state. The differences arise from the change in coordinations; Thr35 binds to Mg^{2+} in state 2, whereas the coordination is broken in state 1 and the GDP-bound state. The absence of the coordinations results in not only the distortions but also the large fluctuation of switch I in state 1. The present result suggests that the distortion caused by the breaking of the coordinations in switch I weakens affinities with effectors in state I.

In switch II, we found no significant difference between the secondary structure in states 1 and 2 because the coordinations in the region are conserved in these states. In contrast, structural change between the GTP- and GDP-bound states, arising from the breaking of the HB between γ-phosphate and Gly60, is found and Gly60 and its neighbor residues adopt an extended form in the GDP-bound state. Large fluctuations are experimentally found in switch II in GTP-bound state. As experimental results, large fluctuations in the α2 helix, the transitions among 3_{10}-helix, α-helix, and a partially unwound helix are found in states 1 and 2, on the other hand, any significant fluctuation in α2 helix is not seen in the GDP-bound state. We found that the fluctuations are correlated with the rearrangement of transient HBs involving the polar side-chains in switch II in the states 1 and 2. The present result implies that conformations in fluctuation are stabilized by transient HBs, so that interconversions among multiple states take place in GTP-bound state.

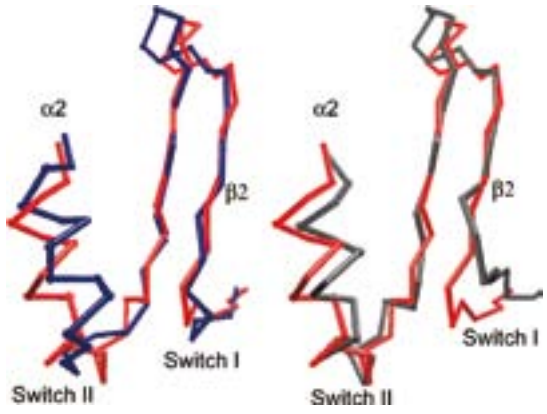

Figure 1. Superposition of the average Cα traces in switches I and II, and the neighbor region in state 1 (gray), state 2 (red), and GDP-bound state (blue), respectively.

3. Ultrafast Intermolecular Dynamics of Liquid Water: Theoretical Study of Two-Dimensional Infrared Spectroscopy

Physical and chemical properties of liquid water are dominated by hydrogen bond structure and dynamics. Recent studies of nonlinear vibrational spectroscopy of intramolecular motion provide new insight into ultrafast hydrogen bond dynamics. However, our understanding of intermolecular dynamics of water is still limited. In this study, we theoretically investigated intermolecular dynamics of liquid water in terms of two-dimensional infrared (2D IR) spectroscopy. We calculated the 2D IR spectrum by explicitly estimating the three-time correlation function of the total dipole moment, and thus obtained novel information about the time dependent mode couplings that cannot be available from the one-dimensional spectroscopy (Figure 2).

We found that the frequency correlation, *i.e.* the initial inhomogeneity, of the libration motion is lost with the time scale of ~110 fs. The energy of the libration motion relaxes to the low frequency motion with the time scale of ~80 fs. The energy relaxation to the low frequency motion is followed by the slow relaxation due to the hydrogen bond structural change induced by incident electric field pulses. We analyzed the effect of the hindered translation motion on these ultrafast dynamics. It was shown that both the frequency modulation of libration motion and the energy relaxation from the libration to the low frequency motion significantly slow down in the absence of the hindered translation motion. The present result revealed that the anharmonic coupling between the hindered translation and libration motions is essential for the ultrafast relaxation dynamics in liquid water.

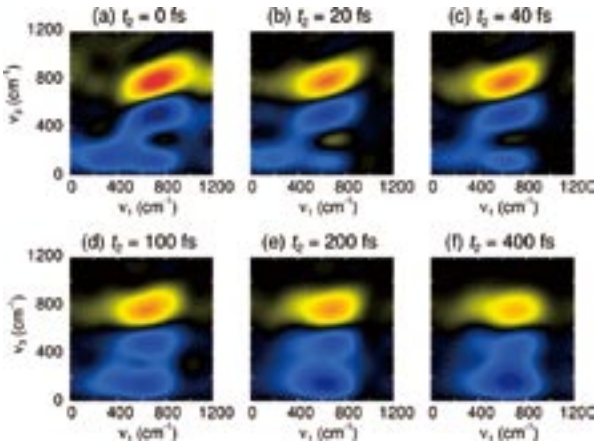

Figure 2. 2D IR correlation spectra of intermolecular motion of liquid water at several waiting times. The positive peak at (ν_1,ν_3) = (~700 cm^{-1},~800 cm^{-1}) is due to the stimulated emission and the bleaching of the libration motion and the negative peak at (~700 cm^{-1},~500 cm^{-1}) is due to the excited state absorption.

Reference

1) T. Yagasaki and S. Saito, J. *Chem. Phys.* **128**, 154521 (7 pages) (2008).

Theoretical Study on Molecular Excited States and Chemical Reactions

Department of Theoretical and Computational Molecular Science
Division of Computational Molecular Science

EHARA, Masahiro Professor
KAWAGUCHI, Ritsuko Secretary

Molecules in the excited states show characteristic photophysical properties and reactivity. We investigate the molecular excited states and chemical reactions which are relevant in chemistry, physics, and chemical biology with developing the highly accurate electronic structure theory. We are also interested in the excited-state dynamics and energy relaxation so that we also develop the methodology of large-scale quantum dynamics. In this report, we report our recent studies on the inner-shell spectroscopy[1,2] and catalytic reaction.[3]

1. Theoretical Study of the Vibration-Induced Suppression of Valence-Rydberg Mixing[1]

The vibrational wave function of a molecule is spatially more spread out when the molecule has one or more quanta of vibrational excitation. Thus spectroscopic studies of vibrationally excited molecules can be used to probe different regions of the potential surfaces of electronically excited states. In this work, we examine that vibrational excitation of the electronic ground state significantly affects the amount of valence character observed in the Rydberg series in the x-ray absorption spectrum of N_2O. In the O1s x-ray absorption spectrum of ground state N_2O, the ns σ Rydberg series appears with significant intensity due to a mixing of σ* valence character in the Rydberg states. But, the excitation of the Rydberg states is significantly suppressed for ground state molecules in excited bending-mode vibrational states.

Figure 1 compares the initial-state specific ARIY (Angle-Resolved Ion Yield) spectra in the vicinity of the O 1s ionization threshold. The absorption spectra were observed at 300/700 K and the vibrationally excited absorption spectrum was extracted assuming the Boltzmann distribution. A key finding is that the intensity of the *ns* σ Rydberg series and *A*' state are significantly suppressed and increased for excitation from vibrationally excited states, respectively, whereas the intensity of the *ns* σ Rydberg series is unchanged. These observations suggest that the decrease in the bond angle causes a decrease in the mixing in of valence character that enhances the transition probability to the Rydberg states. In order to understand these phenomena, we executed the SAC-CI calculations of the energies and the second moment $\langle r^2 \rangle$ of the O1s excited states varying the bond angle.

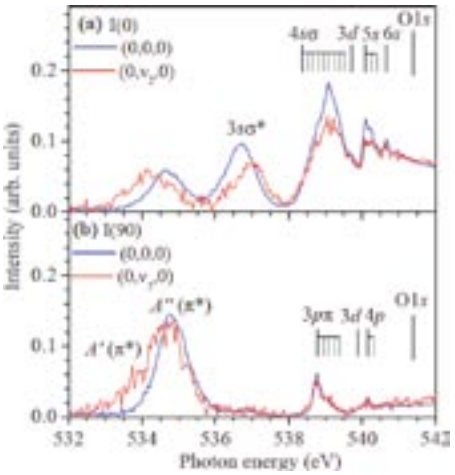

Figure 1. ARIY spectra in the N_2O O1s π* and Rydberg excitation region. (a) Initial state specific 0°ARIY spectra for the vibrationally ground state (blue) and vibrationally excited states (red). (b) Initial state specific 90°ARIY spectra.

Figure 2 shows cuts of the calculated potential energy surfaces of the O 1s excited states of *A*' symmetry. The 1*A*' state is correlated to the π* state and stabilizes along the bending coordinate. All other states are stable in the linear structure. A characteristic curve crossing occurs between the σ and π Rydberg states along the bending coordinate. These potential curves explain the red shift of the π* state and the blue shift of 3sσ and 4sσ states. In order to analyze the mixing of the valence character in the Rydberg states, we examined the electronic part of the second moment $\langle r^2 \rangle$, which is anticorrelated to the amount of valence character (Figure 3). The second moments of the 3sσ, 4sσ, and 5sσ states become large as the molecule becomes bent. This indicates that the

mixing of the valence character in these states becomes less as the bond angle decreases. Consequently, the absorption oscillator strength to the *ns* σ Rydberg states becomes small. These results confirm the interpretation of the intensity changes observed for excitation from vibrationally excited molecules.

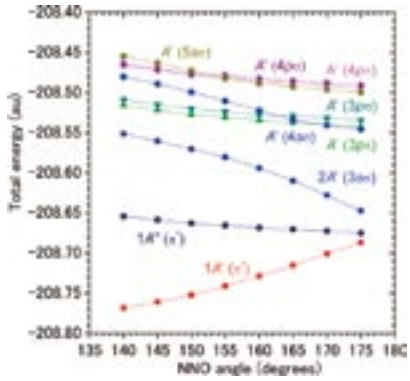

Figure 2. Potential energy curves of the low-lying O1s excited states of N_2O at R_{NN} = 1.127 Å and R_{NO} = 1.185 Å.

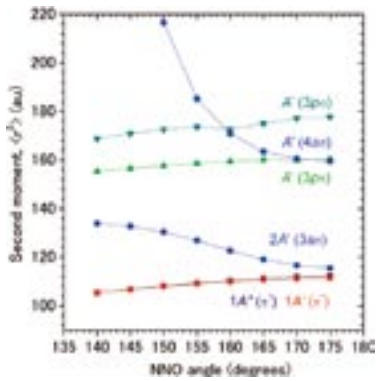

Figure 3. Second moments $\langle r^2 \rangle$ of the low-lying O1s excited states of N_2O at R_{NN} = 1.127 Å and R_{NO} = 1.185 Å.

As seen in Figure 2, the 1*A*'(π*) state stabilizes along the bending coordinate whereas the 2*A*'(3*s*) state destabilizes more than the 1*A*"(π*) state. This anticorrelation indicates that the 1*A*'(π*) and 3*sA*' states are strongly coupled. We believe that this coupling opens a flow of the valence character from the 3*sA*', 4*sA*', and 5*sA*' Rydberg states to the 1*A*'(π*) state. Analyzing the MOs which contribute to the excitations, we concluded that the counterpart of the decrease in the mixing of the valence character in the 3*s*, 4*s*, and 5*s* states is an increase in the *s*σ -type character of the *a*'(π*) orbital.

Thus, using an *ab initio* analysis of the electronic part of the second moment $\langle r^2 \rangle$, the suppression is interpreted as being due to a decrease in the mixing of the valence character in the *ns* σ Rydberg states with decreasing bond angle.

2. Theoretical Study of the Palladium-Catalyzed Regioselective Silaboration of Allene[3)]

Transition-metal catalyzed additions of silicon-containing σ-bonds to unsaturated bonds of organic molecules have been a major strategy for the synthesis of organosilicon compounds. While Si–Si bond addition has been extensively studied, addition reactions involving silicon–heteroatom bonds such as B, Sn and Ge have become important topics in recent years. Many reactions of these interelement σ-bonds proceed regioselectively, leading to the effective syntheses of regiodefined organosilicon compounds. Recently, effective silaboration reactions of allenes using silylborane have been developed. These reactions proceed in a regio- and stereoselective fashion in the presence of the palladium catalyst, producing synthetically useful β-borylallylsilanes in high yields.

We theoretically investigated this catalytic reaction, the silaboration of allene catalyzed by the Pd complex, to clarify the reaction mechanism and the origin of the regioselectivity (Figure 4). We examined the overall reaction scheme in particular to determine the mechanism of the regioselectivity. The present catalytic reaction is exothermic and the rate-determining step is the insertion of allene into the Pd–B bond of the Pd complex. σ-Allylic and π-allylic complexes exist as intermediates and play an important role in the regioselectivity. Selective insertion of the unsubstituted C=C bond into the Pd–B bond produces the most stable σ-allylic complex, which converts to the π-allylic complex while maintaining the Pd–O coordination. The selective formation of the specific σ-allylic complex and the large activation barrier between two isomeric π-allylic complexes dominantly determines the regioselectivity of the present reaction. The major-product complex is less stable than the minor-product complex, and therefore kinetic control is predominant in the present reaction.

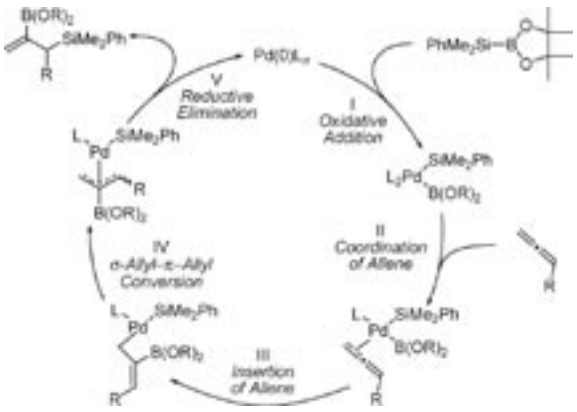

Figure 4. Reaction mechanism of the palladium-catalyzed regioselective silaboration of allene.

References

1) T. Tanaka, M. Hoshino, H. Kato, M. Ehara, N. Yamada, R. Fukuda, H. Nakatsuji, Y. Tamenori, J. R. Harries, G. Prümper, H. Tanaka and K. Ueda, *Phys. Rev. A* **77**, 012709 (4 pages) (2008).

2) M. Ehara and H. Nakatsuji, *Collect. Czech. Chem. Commun.* **73**, 771–785 (2008).

3) Y. Abe, K. Kuramoto, M. Ehara, H. Nakatsuji, M. Suginome, M. Murakami and Y. Ito, *Organometallics* **27**, 1736–1742 (2008).

Theory and Computation of Liquids and Liquid Interfaces

Department of Theoretical and Computational Molecular Science
Division of Computational Molecular Science

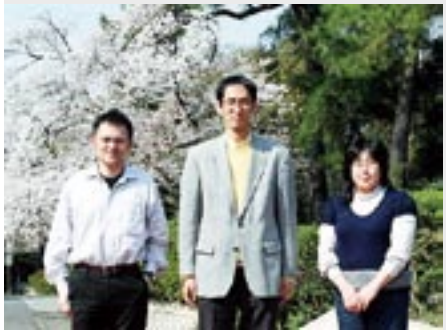

MORITA, Akihiro	Professor*
ISHIDA, Tateki	Assistant Professor
KAWAGUCHI, Ritsuko	Secretary

The following projects 1 and 2 focus on the development of theory and computational analysis methods for interfacial sum frequency generation (SFG) spectroscopy and its application to aqueous interfaces. The visible-infrared sum frequency generation spectroscopy is a powerful method to obtain interface-specific vibrational spectra. While this experimental technique is now widely used as an interface probe in a molecular level, reliable interpretation of the observed spectra is often lacking which significantly hinders the progress of this surface characterization method. The following project 1 summarized the theoretical methods of SFG analysis that we have developed. Project 2 is a collaborative work with experimental groups of Drs. Miyamae at AIST and Dr. Ouchi at Nagoya. Collaboration of SFG experiments and the theoretical analysis will be a powerful way to study liquid interfaces. Project 3 summarizes theoretical study of mass transfer dynamics and kinetics at liquid-water interfaces.

Projects 4, 5, and 6 are mainly conducted by Dr. Ishida and his collaborators.

1. Theory of Sum Frequency Generation Spectroscopy[1)]

Gas-liquid interfacial structures of NaCl and NaI aqueous soluThis article summarizes computational analysis of the vibrational Sum Frequency Generation (SFG) spectroscopy with molecular dynamics simulation. The analysis allows direct comparison of experimental SFG spectra and microscopic interface structure obtained by molecular simulation, and thereby obviates empirical fitting procedures of observed spectra. In the theoretical formulation, the frequency-dependent nonlinear susceptibility of an interface is calculated in two ways, based on the energy representation and time-dependent representation. The application to aqueous interfaces revealed a number of new insight into the local structure of electrolyte interfaces and interpretation of the SFG spectroscopy.

2. Sulfuric Acid Aqueous Solution Surfaces Studied by a Combination of Sum Frequency Generation and Molecular Simulation[2)]

This project is a collaborative work with experiment of SFG spectroscopy. The vibrational sum frequency generation spectra of the air-liquid interface of H_2SO_4-H_2O solutions over the wide range of concentration are measured in the SO stretch region (1000–1300 cm^{-1}). This is the first measurement of sulphur species at the surface region with distinguishing their ionization state. The analogy of the concentration dependence of Raman and SFG is indicative of a nearly identical behavior of the first acid dissociation at the air-liquid interface as in the bulk.

3. Theoretical Investigation of Aqueous Surface Structure and Mass Transfer Dynamics[3)]

The mass transfer mechanism across gas/water interface is studied with molecular dynamics (MD) simulation. The MD results provide a robust and qualitatively consistent picture to previous studies about microscopic aspects of mass transfer, including interface structure, free energy profiles for the uptake, scattering dynamics and energy relaxation of impinging molecules. These MD results are quantitatively compared with experimental uptake measurements, and we find that the apparent inconsistency between MD and experiment could be partly resolved by precise decomposition of the observed kinetics into elemental steps. Remaining issues and future perspectives toward constructing a comprehensive multi-scale description of interfacial mass transfer are summarized.

4. Theoretical Study of Temperature and Solvent Dependence of the Free-Energy Surface of the Intramolecular Electron-Transfer Based on the RISM-SCF Theory[4)]

The free-energy surfaces along the intramolecular electron-transfer reaction path of the 1,3-dinitrobenzene radical anion in acetonitrile and methanol are investigated with the reference interaction site model self-consistent field theory. Although acetonitrile and methanol have similar values of the dielectric constant, the free-energy profiles are quite different. In the methanol solution, the charge is strongly localized on one of the nitrile substituents due to a strong hydrogen bond between 1,3-dinitrobenzene and the solvent, while the polarization is not so large in the case of acetonitrile. The temperature dependence of the reorganization energy, the coupling strength, and the activation barrier decrease with increasing temperature for both cases. The electronic coupling strength also shows a similar tendency in the temperature dependence; it increases with increasing temperature in both solvents but with different rates. The behavior is explained in terms of the strong polarization induced by the hydrogen bond between the solute and solvent in the methanol solution.

5. Optimal Charge and Charge Response Determination through Conformational Space: Global Fitting Scheme for Representative Charge and Charge Response Kernel[5)]

We propose global fitting scheme derived in least-square sense to estimate optimal partial charge and charge response kernel (CRK), $\partial Q_a/\partial V_b$, with the data collected from conformational space sampling. We applied the global fitting method to 1-butanol system and the performance and accuracy of our global fitting procedure are shown. In addition, we choose 1-pentanol as the test system with the electronic structure change via conformational change and applied the global fitting method to it. From our study, it is indicated that intramolecular polarization can be influenced by intramolecular hydrogen bonding, and it is shown that our global fitting method can correspond to such situation. Also, the global fitting procedure is tested in a large molecular system, 1-dodecanol. We show the results of the availability of our fitting method for the system needed to sample large sets of data over large conformational space. It is indicated that the nonlocality in intramolecular polarization in alkyl chain sequence can be observed and that the large fluctuation of CRKs via nonbonded interaction such as intramolecular hydrogen bonding, as seen in the 1-pentanol case, can appear in common. The global fitting scheme we proposed is available for building molecular modeling considering polarization effect explicitly even in the case that target systems include a lot of conformers.

6. Theoretical Study of Strong Coupling between Solvation and Electronic Structure in the Excited State of a Betaine Dye[6)]

The electronic ground and excited state structures of the betaine dye molecule pyridinium-N-phenoxide [4-(1-pyridinio) phenolate] are investigated both in the gas phase and in aqueous solution, using the reference interaction site model self-consistent-field (RISM-SCF) procedure within a CASSCF framework. We obtain the total free energy profiles in both the ground and excited states with respect to variation in the torsion angle between the phenoxide and pyridinium rings. We analyze the effect of solvent on the variation of the solute dipole moment and on the charge transfer character in the excited state. In the gas phase, it is shown that the potential energy profile in the excited state decreases monotonically toward a perpendicular ring orientation and the dipole moment decreases along with decreasing charge localization. In water, the free energy surface for twisting is better characterized as nearly flat along the same coordinate for sterically accessible angles. These results are analyzed in terms of contributions of the solvation free energy, the solute electronic energy, and their coupling. Correspondingly, the dependence of the charge transfer character on solute geometry and solvation are analyzed, and the important roles in the excitation and subsequent relaxation processes for the betaine dye are discussed. It is found that there is considerable solute electronic reorganization associated with the evolution of solvation in the excited state, and it is suggested that this reorganization may contribute significantly to the early time evolution of transient spectra following photoexcitation.

References

1) A. Morita and T. Ishiyama, *Phys. Chem. Chem. Phys.* in press (2008).
2) T. Miyamae, A. Morita and Y. Ouchi, *Phys. Chem. Chem. Phys.* **10**, 2010–2013 (2008).
3) A. Morita and B. J. Garett, *Flu. Dyn. Res.* **40**, 459–473 (2008).
4) N. Yoshida, T. Ishida and F. Hirata, *J. Phys. Chem. B* **112**, 433–440 (2008).
5) T. Ishida, *J. Phys. Chem. A* **112**, 7035–7046 (2008).
6) T. Ishida and P. J. Rossky, *J. Phys. Chem. B* **112**, 11353–11360 (2008).

* Present Address; Department of Chemistry, Graduate School of Science, Tohoku University, Aoba-ku, Sendai 980-85788

Visiting Professors

Visiting Professor
AIDA, Misako *(from Hiroshima University)*

Topological Analysis of Water Clusters

A water cluster is relevant to a digraph and can be classified to an H-bond pattern. The NVT ensembles of water clusters are created and divided into the configurational subsets, which correspond to the topology-distinct H-bond patterns, and the relative molar Helmholtz energies of the H-bond patterns are evaluated. The method is based on the combination of the standard Monte Carlo techniques with defined H-bond patterns. The structure distributions of water clusters at different temperatures are presented based on the H-bond patterns instead of the 'inherent structures.' The thermodynamically favored structures of water clusters, which are energetically favored and readily feasible (entropy-favored for cluster formation), are presented. The aim of the present work is to demonstrate that the classification to the H-bond pattern corresponds to the division of the configurational space of water cluster structures, where the H-bond patterns can be used to distinguish water cluster structures at finite temperatures created by a simulation technique.

Visiting Associate Professor
NISHINO, Masamichi *(from National Institute for Materials Science)*

Elucidation of the Mechanism of Photoinduced Phase Transitions in Molecular Solids

The discovery of LIESST (light-induced excited spin state trapping) phenomena has accelerated studies of functional spin-crossover (SC) molecular solids. SC compounds have been studied intensively not only because of their potential applicability to novel optical devices, *e.g.*, optical data storage and optical sensors, *etc.*, but also because of the fundamental scientific interest in the mechanism of the phase transition and the accompanied nonlinear relaxation processes. Focusing on such novel phenomena, through the development of theoretical and computational methods, I am studying the properties of cooperative effects which are the key to understand the mechanism of the photoinduced phase transition.

Visiting Associate Professor
KITAO, Akio *(from The University of Tokyo)*

Theoretical Study on Dynamics and Function of Biopolymer and Biological Supramolecule

Recently, rapid progress in computational power and algorithms enable us to carry out massive molecular simulations of biomolecular systems in longer time scale than before. Proteins are essential molecules that manage various chemical reactions in biological systems. Our main targets are proteins, other biopolymers and biological supramolecules, which act as essential functional units in living organisms. We have been studying assembly process, properties and functional mechanisms of biomolecules using theoretical and computational approaches. In order to achieve this, we create new computational methodologies and programs to simulate biomolecular systems more realistically and accurately and use them to investigate atomic mechanisms of supramolecules to fold, assemble and function. We also develop methodology to extract useful information from experimental data and analyze molecular mechanisms to function. In addition, we analyze accumulated information on protein structure and function and store it as databases.